Main Article

Progress in Physical Geography
2025, Vol. 0(0) 1–19

DOI: 10.1177/03091333251320817
journals.sagepub.com/home/ppg
Sage

Sources and concentration of DOC, DIC, and POC in the Lianjiang River: A representative karst tributary of the Beijiang River

Zuobing Liang
Key Laboratory of Karst Dynamics, MNR & Guangxi, Institute of Karst Geology, CAGS, Guilin, China

School of Geography and Planning, Sun Yat-sen University, Guangzhou, China

Jiangxi Provincial Key Laboratory of Carbon Neutrality and Ecosystem Carbon Sink, Lushan Botanical Garden, Jiangxi Province and Chinese Academy of Sciences, Jiujiang, China

Pengcheng Zhang*, Rui Li, Qirui Wu, Zaizhi Yang, Di Tian and Shaoheng Li
School of Geography and Planning, Sun Yat-sen University, Guangzhou, China

Kun Ren
Key Laboratory of Karst Dynamics, MNR & Guangxi, Institute of Karst Geology, CAGS, Guilin, China

School of Geography and Planning, Sun Yat-sen University, Guangzhou, China

Yuchuan Sun
Key Laboratory of Karst Dynamics, MNR & Guangxi, Institute of Karst Geology, CAGS, Guilin, China

Chongqing Key Laboratory of Karst Environment, School of Geographical Sciences, Southwest University, Chongqing, China

Jianhong Li
Key Laboratory of Karst Dynamics, MNR & Guangxi, Institute of Karst Geology, CAGS, Guilin, China

Abstract

Isotopic compositions of $\delta^{13}C_{DIC}$, sources and abundance of dissolved inorganic carbon (DIC), dissolved organic carbon (DOC), particulate organic carbon (POC), and their response to hydrologic regimes were examined from Lianjiang River stream in rainy (DIC and DOC) and dry seasons (DOC and POC). Lianjiang

*Pengcheng Zhang contributed equally to this work and should be considered co-first authors.

Corresponding authors:
Zuobing Liang, Key Laboratory of Karst Dynamics, MNR & Guangxi, Institute of Karst Geology, Chinese Academy of Geological Sciences, NO.50, Qixing Ave, Qixing District, Guilin 541004, China.
Email: liangzb6@mail.sysu.edu.cn

Jianhong Li, Key Laboratory of Karst Dynamics, MNR & Guangxi, Institute of Karst Geology, Chinese Academy of Geological Sciences, NO.50, Qixing Ave, Qixing District, Guilin 541004, China.
Email: jianhonglikarst@163.com

River was recharged by groundwater in dry season, the abundance of DIC was higher than DOC. Apart from DIC concentrations in dry season, DIC and DOC concentrations, and $\delta^{13}C_{DIC}$ showed on spatial variation from upstream to downstream. DIC concentrations in rainy season was higher than those in dry season, while $\delta^{13}C_{DIC}$ in dry season was higher than those in rainy season because of increasing contributions from karst groundwater. Carbonate-sourced DIC contributed from 37.1% to 47.8% with an average of 42.6% of the riverine DIC in rainy season, and contributed from 44.6% to 54.5% with an average of 49.9% of the riverine DIC in dry season. Similar carbonate-sourced and soil CO_2 sourced DIC to Lianjiang River in dry season also indicates that Lianjiang River was recharged by groundwater in dry season. Total n-alkanes concentrations in POM were higher than those in DOM, and anthropogenic n-alkanes concentrations were higher than those in biogenic n-alkanes concentrations. Algae and floating/submerged aquatic plants were the major biogenic sources POM and DOM, but part sampling sites with DOM source from terrestrial plants, aquatic macrophytes sources. Light petroleum input and incomplete fossil fuel burning at high temperature and heavy oil emission were the major source of DOM and POM in Lianjiang River, but the contribution of incomplete fossil fuel burning or heavy oil emission in POM was higher than those in DOM. The results shed light on the characteristics and dynamics of different carbons in typical karstic river.

Keywords
dissolved inorganic carbon, $\delta^{13}C_{DIC}$, dissolved organic carbon, n-alkanes, the Lianjiang River

Introduction

The input of dissolved and particulate carbon from watersheds to oceans is influenced by various fluvial processes (Sun et al., 2015), which have significant impacts on regional and global carbon budgets (Ge et al., 2020; Xue et al., 2017). The significant amounts of terrestrial carbon transported by rivers have a notable impact not only on the carbon cycle of marginal seas but also on crucial biogeochemical processes. Therefore, it is essential to investigate the sources of terrestrial carbon transported by rivers and the factors that control their transport to gain a better understanding of the global carbon cycle and marine biogeochemistry (Beaulieu et al., 2012; Bianchi, 2011; Blair and Aller, 2012; Wang et al., 2012). Terrestrial organic carbon transported by rivers includes both particulate organic carbon (POC) and dissolved organic carbon (DOC), while inorganic carbon transport comprises both particulate inorganic carbon (PIC) and dissolved inorganic carbon (DIC) (Bauer et al., 2013; Cole et al., 2007). The primary sources of organic carbon in most rivers are plants, river algae, soil organic matter, and ancient organic matter released through weathering processes (Armstrong, 2012; Mayorga et al., 2005). And DIC is predominantly composed of bicarbonate ions, which primarily originate from the chemical weathering of carbonates and silicates within the river's drainage basin (Chen et al., 2021). However, the contribution of anthropogenic sources to organic matter in POM and DOM in river systems remains unclear.

The transport of riverine organic and inorganic carbon is influenced by various complex factors, such as landform, soil type, vegetation condition, and fluvial processes. However, previous studies have mostly focused on the seasonal dynamics of dissolved inorganic carbon (DIC) and dissolved organic carbon (DOC) in rivers, with little attention given to investigating the seasonal variations of DIC and DOC in river water and their interactions with groundwater. Groundwater can act as a source of river water and DIC or DOC, which are controlled by hydrologic regimes such as flow paths and connectivity (Larsen et al., 2010; Singh et al., 2014; Yang et al., 2020). Groundwater accounts for 95% of the liquid freshwater on Earth and contains a diverse array of dissolved organic matter (DOM) molecules that play a crucial role in the global carbon cycle. Recent research suggests that the extraction of groundwater and the discharge of subterranean groundwater to oceans could lead to the release of up to 13 Tg of highly photolabile and aerobically

biolabile DOC from groundwater to surface environments annually, where it can be rapidly degraded (McDonough et al., 2022). Karst areas cover approximately 15% of the Earth's land surface and have a significant impact on terrestrial carbon uptake and environmental quality (Liu et al., 2018), and the reservoirs in karst areas play a crucial role in the global carbon cycle (Beaulieu et al., 2012). Karst water bodies provide more favorable conditions for the biological carbon pump (BCP), making it essential to understand the reservoir effect in karst areas on a global scale in terms of the carbon cycle (Liu et al., 2018). In general, it is necessary to investigate the sources and distributions of organic and inorganic carbon in karst river water.

DIC sources in river water primarily originate from soil CO_2 (via groundwater), atmospheric CO_2 exchange, planktonic respiration, chemical weathering, and the dissolution of carbonate rocks. DIC concentrations are then influenced by water-air CO_2 exchange processes, hydrologic inputs, vegetation, and carbonate weathering. The stable isotope composition of DIC ($\delta^{13}C_{DIC}$) is largely determined by the isotope balance between carbonate minerals and soil CO_2, as well as the isotope exchange between soil CO_2 and soil DIC (Hao et al., 2019; Liu and Han, 2020; Peterson and Fry, 1987). This composition is valuable for tracing DIC sources and understanding the factors affecting DIC levels in river water. n-Alkane are one of the most abundant lipid molecules biosynthesized by terrestrial plants, aquatic plants, and planktons, due to their ubiquitous presence and diagenetic and chemical stability, which have long and successfully been used in assessing the sources and fate of OM in natural environments (Derrien et al., 2017; Ficken et al., 2000a). Hydrological isotopes, such as oxygen and hydrogen, provide valuable information about water sources and processes. On one hand, isotopic fractionation occurs during processes like evaporation, condensation, and precipitation. By analyzing isotopic ratios in water samples, researchers can determine how these processes affect the water, offering insights into its origin and movement. On the other hand, different hydrologic inputs (e.g., rainwater, snowmelt, and groundwater) have distinct isotopic compositions. By comparing the isotopic ratios of water samples with known sources, researchers can trace the contributions of various inputs to a specific water body (Gat et al., 1996). Thus, the unique isotopic signatures and fractionation patterns of oxygen and hydrogen make them powerful tools for tracing and understanding hydrologic inputs. And the use of carbon isotopes, hydrology isotopes, and lipid biomarkers will provide insights into the sources and transport mechanisms of carbon within the river system. Carbon isotopes will help trace the origins of DIC, hydrology isotopes will elucidate the role of groundwater in carbon transport, and lipid biomarkers will identify the specific organic sources contributing to POM and DOM.

The Lianjiang River Basin is the largest karst area in Guangdong Province, characterized by a typical subtropical monsoonal climate and a continuous outcrop of carbonate rocks. Few studies have investigated the temporal variability of carbon dynamics in karstic rivers, particularly in the Lianjiang River Basin. This study hypothesizes that the spatial and temporal variations in DIC concentration and carbon isotopic composition in the Lianjiang River are influenced by both natural processes, such as chemical weathering and biological activity, and anthropogenic factors, such as land use and water management practices. Therefore, this study aimed to evaluate the spatial and temporal variations in the concentration and carbon isotopic composition of dissolved inorganic carbon (DIC) using chemical techniques and to investigate the sources of particulate organic matter (POM) and dissolved organic matter (DOM) influenced by hydrologic regimes in the dry season using lipid biomarkers.

Materials and methods

Site description

The Lianjiang River, the largest tributary of the Beijiang River, is located in the northwest of Guangdong Province. The Lianjiang River Basin, spanning 10,061 km^2, lies within the subtropical monsoon zone of southern China. This region experiences a mean annual temperature of 19 to 20°C and receives an average annual rainfall of 1770 mm, primarily between April and June. The basin's geology is diverse, with carbonate rocks, predominantly limestone, making up approximately 60% of the area's outcrop. The parent material for soil formation in the basin is primarily pure limestone, with occasional occurrences of marlstone and siliceous limestone. Consequently, limestone soil is the dominant zonal soil type in the study area,

representing a typical lithosol developed from limestone. This soil type is extensively and continuously distributed throughout the region (Figure 1).

In the upper soil layers, calcium carbonate is leached, while clay particles and iron-aluminum oxides migrate and accumulate within the profile. The accumulation layer and subsoil have a relatively heavy texture, ranging from clay loam to clay. The soil exhibits a blocky structure, with noticeable clay coatings on the surfaces, and occasionally, pea-like iron-manganese nodules are present. The vegetation of the Lianjiang Basin is dominated by C3 vascular plants, with subtropical evergreen broadleaf forests widely distributed across the area. The flora is diverse, with the majority of species belonging to the *Fagaceae, Theaceae, Asteraceae, Rosaceae*, and *Fabaceae* families.

Sampling and analysis

River water samples (n = 18) from Lianjiang River were collected in rainy season (August 2021, n = 8) and dry season (April 2022, n = 10). The river water was sampled using a stainless-steel sampler at least 1 m from the river bank. The water temperature, pH and electrical conductance (EC) were measured in situ by using HACH portable meters (HQ40d). Water samples were filtered using 0.22-μm pore size membrane filters (Millipore) to remove suspended particles and microorganisms, after which major cation samples were immediately acidified to pH<2 with hydrochloric acid. Samples for $\delta^{13}C_{DIC}$ were collected in 25 mL acid-washed dry HDPE bottles and three drops of saturated $HgCl_2$ were added to prevent microbial activity. The remaining water samples were stored at 4°C under dark conditions upon arrival at the laboratory. Top soil (0~5 cm depth) samples (n = 18) were collected by stainless-steel spade. Soil samples were oven-dried at 100–105°C before the < 2 mm fraction was separated by grinding and sieving. All visible roots, which were not numerous, were removed both prior to and following grinding and sieving. Calcium carbonate

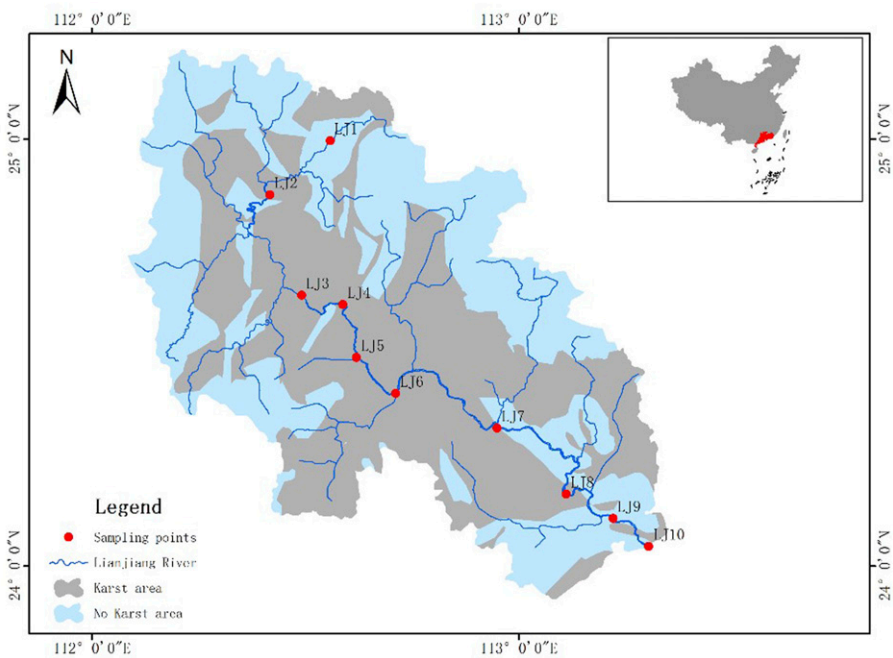

Figure 1. Map of selected sampling sites. For interpretation of the references to colours in this figure legend, refer to the online version of this article.

was eliminated by leaching with 1N HCl in an ultrasonic bath until effervescence ceased and a low pH was obtained. Rock samples (n = 3) were taken from drill cuttings. Samples for n-Alkanes (n = 10) were collected in 4 L pre-combusted (at 450°C in Muffle furnace) brown glass bottles (screw cap, solid top with PTFE liner) and three drops of saturated $HgCl_2$ were added to prevent microbial activity. Water samples (n = 18) for dissolved organic carbon (DOC) analysis were filtered in situ through a 0.22 μm hydrophilic membrane filter into polypropylene sample tubes (50 mL). The remaining water samples were stored at 4°C under dark conditions upon arrival at the laboratory.

A 4 L water sample for n-alkane analysis was filtered through pre-extracted Whatman GF/F glass-fiber filter (effective pore size, 0.7 p.m.) at low vacuum using a Millipore filtration system. The filtrate was acidified to pH = 2 and extracted with dichloromethane:methanol (3:1) using ultrasound-assisted extraction. After extraction, the majority of the water was discarded, and the organic fraction was separated in a separatory funnel. Small quantities of methanol were added to break up any emulsions. The POM and DOM extracts were concentrated by rotary evaporation, and the resulting concentrated extracts were saponified (1 KM) and extracted with hexane: dichloromethane (4:1, 4 × 10 mL) to obtain the neutral fractions. Subsequently, these were further fractionated by silica column chromatography to isolate the aliphatic hydrocarbons.

Analytical procedures

All major ions (Cl^-, NO_3^-, and SO_4^{2-}) except HCO_3^- (which was titrated immediately in the field using a portable testing kit made by Merck KGaA Co., Darmstadt, Germany, with an accuracy of 0.05 mmol/L) were analyzed using a DX-600 ion chromatograph with a detection limit of 0.1 ppm. Major cations were analyzed by inductively coupled plasma optical emission spectrometry (Optima 8300, Perkin-Elmer, USA) with a detection limit of 0.05 ppm for Ca^{2+}, Mg^{2+}, K+, Na^+, in the laboratory. DOC were analyzed by catalytic combustion using a Shimadzu TOC-L analyzer (TOC-V cph/cpn: Shimadzu Corporation, Kyoto, Japan). Furthermore, in this study, we found no significant difference in the reproducibility (standard deviation) of ion and DOC measurements ($p > 0.5$).

Carbon isotopes. $\delta^{13}C_{DIC}$ values were analyzed using a MAT-253 mass spectrometer coupled with a Gas Bench II automated device with analytical precision of ± 0.15‰, the results are expressed as $\delta^{13}C_{DIC}$ (‰) with respect to the Vienna Pee Dee Belemnite (V-PDB) standard, and carbon isotope analysis were carried out at the Environmental and Geochemical Analysis Laboratory of the Institute of Karst Geology, Chinese Academy of Geological Sciences. The precision of the mass spectrometric measurements was ± 0.1‰. The $\delta^{13}C$ values for the soils and carbonate rocks were determined by analysis using a Finnigan MAT Delta-S mass spectrometer at the Environmental and Geochemical Analysis Laboratory of the Institute of Karst Geology, Chinese Academy of Geological Sciences. The precision of the mass spectrometric measurements was ± 0.1‰.

Hydrology isotopes. Stable isotope ratios of hydrogen and oxygen were measured using the cavity ring-down laser spectroscopy method with a Picarro L2121-i isotope water analyzer in the laboratory of the School of Environmental Science and Engineering, Sun Yat-sen University. Hydrogen and oxygen isotope ratios were expressed in per mille (‰) relative to Vienna Standard Mean Ocean Water. Reproducibility of stable isotope measurements was ± 0.1‰ for $\delta^{18}O$ and ± 1‰ for δD.

Biomarkers. The n-alkanes were analyzed by GC-MS, the procedural blanks were carried throughout, no significant lipid contamination was observed. The extract was blown down to 1 mL under a gentle flow of nitrogen, and then analyzed by gas chromatography–mass spectrometry (GC–MS, Agilent 7890A GC, 5975C MSD) in selected ion monitoring (SIM) modes with internal standards n-Alkanes, and Deuterated tetracosane was used as internal standard for quantifying (Liang et al., 2022). In addition, the standard deviation of the measured standard n-alkanes (C13–C38) in all three trials showed no any significant differences in the reproducibility of the measured n-alkanes (p >0.7).

Calculation of SI_C, SI_D, *and* PCO_2. The complete hydrochemical data sets, including recorded temperature and pH, as well as calculated values for Ca^{2+}, Mg^{2+}, and HCO_3^-, along with the values of K^+, Na^+, Cl^-, and SO_4^{2-}, were processed using the WATSPEC program (Wigley, 1977), which calculates SI_C, SI_D, and PCO_2 (Li et al., 2008; Pu et al., 2014).

Qualitative assessment of biomarker. Anthropogenic activities and biogenic input were considered as two main contributors to the presence of n–alkanes in the environment (Zheng et al., 2000), and anthropogenic and biogenic n-alkanes were distinguished by subtraction by using the following equations (Caumo et al., 2020; He et al., 2020):

$$\text{bio } C_n = Cn\text{-}[(C_{n-1} + C_{n+1})]/2$$

$$\text{anthro } C_n = C_n\text{-} \textit{ bio } C_n$$

where n refers to the carbon-chain number, and n is odd. C_n, C_{n-1}, and C_{n+1} stand for n-alkanes which carbon-chain number of n, n–1, and n + 1, respectively, anthroC_n and bioC_n indicates biogenic and anthropogenic n–alkanes, respectively.

The Kruskal–Wallis test was used to determine if there are statistically significant differences between two or more groups of an independent variable on a continuous or ordinal dependent variable.

Results and discussion

Spatiotemporal variations in the physicochemical parameters of rivers

Oxygen and hydrogen isotopes. In the rainy season, the observed ranges of $\delta^{18}O$ and δ^2H in the Lianjiang River ranged from −6.1‰ to −5.6‰ and from −37.4‰ to −33.4‰, respectively. In the dry season, the isotopic values of Lianjiang River water ranged from −5.9‰ to −5.8‰ for δ^2H and from −35.3‰ to −32.8‰ for $\delta^{18}O$. The isotopic compositions of oxygen in the Lianjiang River did not exhibit significant variation, particularly in the dry season, but a trend toward more enriched $\delta^{18}O$ and δ^2H values was observed (Figure 2). It is interesting to note that the river water samples in the rainy season were grouped above the local meteoric

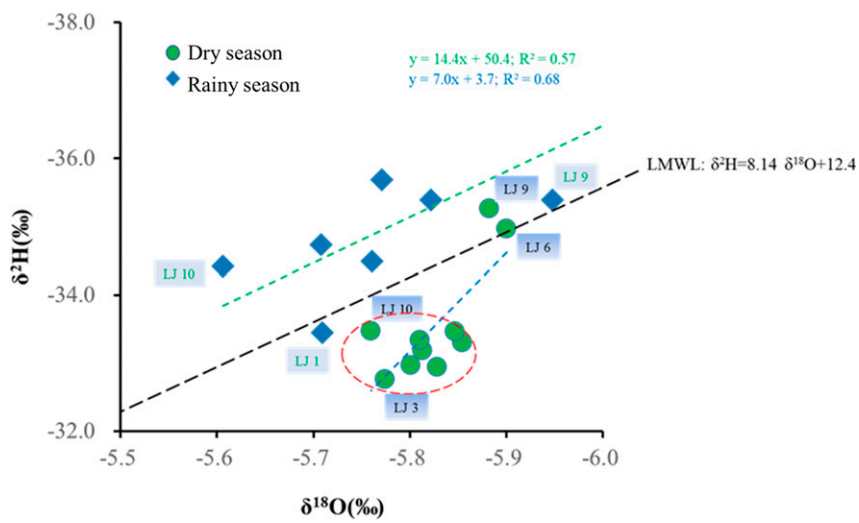

Figure 2. δ^2H-$\delta^{18}O$ plot for river water samples from the study area. For interpretation of the references to colours in this figure legend, refer to the online version of this article.

water line (LMWL), while those in the dry season were below the LMWL based on the δ2H-δ18O relationship in the Lianjiang River. Furthermore, the δ^2H-$\delta^{18}O$ relationship for samples above the LMWL was found to be $\delta^2H = 7.0*\delta^{18}O + 3.7$ in the rainy season and $\delta^2H = 14.4*\delta^{18}O + 50.4$ in the dry season. The scatter of river water samples around the LMWL in the rainy season indicates that the river water was directly recharged by precipitation. However, the higher slope value (14.4) and small variations in δ^2H and $\delta^{18}O$ values in the dry season suggest that the river water was recharged by groundwater. Furthermore, the δ^2H-$\delta^{18}O$ relationship for samples above the LMWL was found to be $\delta^2H = 7.0*\delta^{18}O + 3.7$ in the rainy season and $\delta^2H = 14.4*\delta^{18}O + 50.4$ in the dry season. In the rainy season, the scatter of river water samples around the LMWL indicates that the river water was directly recharged by precipitation. In contrast, the higher slope value (14.4) and small variations in δ^2H and $\delta^{18}O$ values in the dry season suggest that the river water was recharged by groundwater (Li et al., 2015).

DIC, DOC, and $\delta^{13}C_{DIC}$. In the Lianjiang River, the concentration of dissolved inorganic carbon (DIC) ranges between 1.43 and 2.05 mmol/L with an average of 1.89 mmol/L during the rainy season and between 1.91 and 3.12 mmol/L with an average of 2.55 mmol/L during the dry season, with significantly higher DIC concentrations observed in the dry season ($p < 0.05$). This seasonal variation is influenced by the reduced river flow during the dry season, which results in less dilution of weathering products and increased residence time of water, enhancing the DIC concentration. The concentration of dissolved organic carbon (DOC) varies from 0.18 to 0.24 mg/L in the rainy season and from 0.16 to 2.56 mg/L in the dry season. Unlike DIC, DOC concentrations show no significant seasonal variation ($p > 0.05$), indicating that DOC inputs from terrestrial sources and in-stream processing remain relatively stable throughout the year. This stability may be due to consistent organic matter inputs from the surrounding watershed, coupled with the river's ability to process organic carbon efficiently, regardless of seasonal changes in flow.

The $\delta^{13}C_{DIC}$ values, which reflect the isotopic composition of DIC, range from −13.5‰ to −11.2‰ during the rainy season and from −11.2‰ to −9.6‰ during the dry season. The more positive $\delta^{13}C_{DIC}$ values in the dry season ($p < 0.05$) suggest a higher contribution of DIC from carbonate weathering or organic matter degradation, which is less diluted by runoff compared to the rainy season. This isotopic shift also indicates a reduced influence of atmospheric CO_2 dissolution during the dry season, possibly due to lower water temperatures and reduced gas exchange. Additionally, DIC concentrations in the dry season are observed to be higher upstream, gradually decreasing downstream, suggesting that local weathering processes and groundwater inputs are major sources of DIC in the upstream regions. This spatial pattern may reflect the influence of lithology and land use in the upstream catchment areas, where increased carbonate weathering and groundwater contributions are prominent. In contrast, no significant spatial variation is observed in DOC concentrations and $\delta^{13}C_{DIC}$ values along the river, implying that these parameters are more influenced by consistent basin-wide processes, such as the decomposition of organic matter and equilibrium between atmospheric CO_2 and riverine DIC, rather than localized sources (Figure 3).

Overall, riverine DIC concentrations during the rainy season are lower than those in the dry season ($p < 0.05$). This difference can be attributed to the dilution effect of heavy rainfall and floods during the monsoon period (August 2022), which overwhelms the enhanced chemical weathering caused by higher temperatures. The influx of large volumes of runoff during the rainy season leads to a significant dilution of the weathering products, reducing DIC concentrations despite the potential increase in weathering rates due to elevated temperatures (Gao and Wang, 2015).

pCO_2, pH, and saturation index. As shown in Figure 4, almost all of the calcite saturation index (SI_C) and dolomite saturation index (SI_D) values are above 0 during the rainy season, indicating that the river water is supersaturated with respect to calcite and dolomite. This supersaturation suggests that conditions are favorable for the precipitation of these minerals, as the water contains more dissolved calcium carbonate than it can hold in solution. In

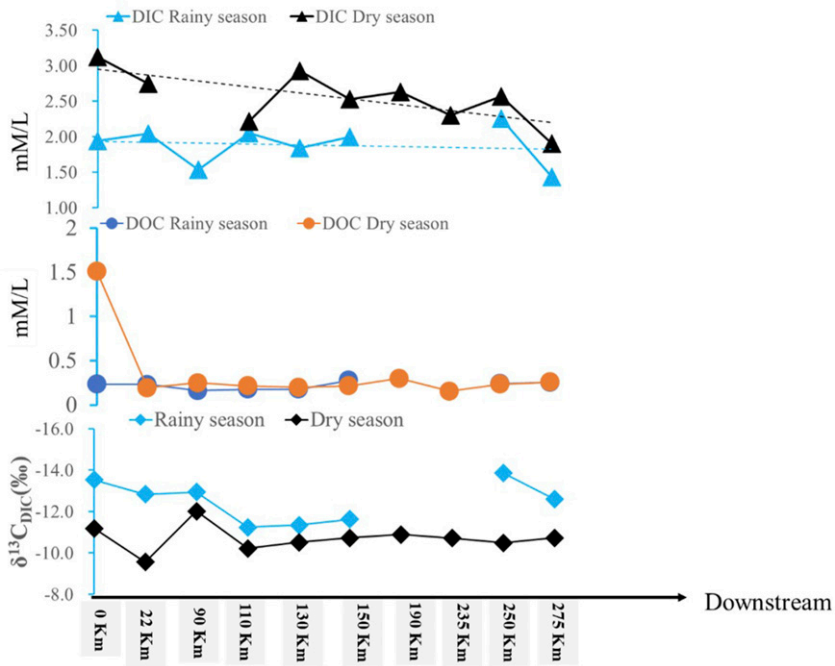

Figure 3. Spatial and seasonal variations of measured variables from the Lianjiang River. For interpretation of the references to colours in this figure legend, refer to the online version of this article.

contrast, all SI_D and SI_C values in the dry season are below 0, indicating that the river water is undersaturated with respect to calcite and dolomite, which promotes the dissolution of these carbonate minerals during the dry season. SI_C and SI_D values in the dry season show a spatial trend, with lower values observed upstream and a gradual increase downstream. This pattern suggests that downstream reaches may experience less carbonate dissolution or potentially some minor precipitation as the water travels further and equilibrates with atmospheric CO_2, thereby slightly increasing its saturation state (Khadka et al., 2014).

In the rainy season, pH values range from 7.6 to 8.6 with an average of 8.1, while in the dry season, pH values range from 6.2 to 7.6 with an average of 7.0. The lower pH values in the dry season ($p < 0.05$) reflect the increased dissolution of carbonate minerals and higher concentrations of CO_2, which acidify the water. This seasonal difference in pH is also linked to the dilution effect during the rainy season, where increased runoff with higher pH dilutes the natural acidity of the river. Moreover, in the rainy season, there is no significant spatial variation in pH values from upstream to downstream, which indicates a consistent buffering capacity throughout the river's course. In the dry season, however, pH values gradually increase from upstream to downstream, suggesting that the river's buffering capacity improves as it moves downstream, likely due to the cumulative effects of carbonate mineral dissolution and reduced CO_2 levels (Andersson et al., 2003).

In the Lianjiang River, partial pressure of carbon dioxide (pCO_2) values in river water range from 389 to 3090 μmol/L, with an average of 1139 μmol/L during the rainy season, reflecting the dilution effect from increased runoff and relatively cooler temperatures that limit CO_2 outgassing. In contrast, pCO_2 values during the dry season are significantly higher, ranging from 8807 to 50,345 μmol/L, with an average of 17,890 μmol/L ($p < 0.05$). This stark increase can be attributed to lower river discharge, prolonged water-soil contact, and enhanced microbial

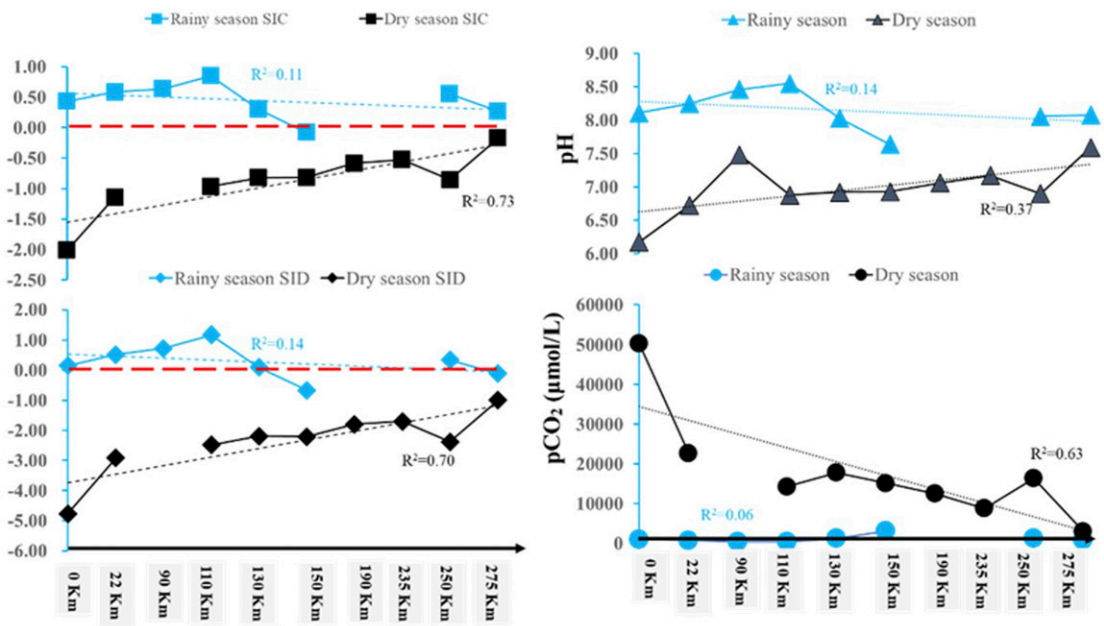

Figure 4. Spatial and seasonal variations values of SI_C, SI_D, pH and pCO_2 in Lianjiang River. For interpretation of the references to colours in this figure legend, refer to the online version of this article.

respiration, which elevates CO_2 levels in the water. The elevated pCO_2 levels in the dry season are a direct result of the reduced flow conditions, which allow for greater accumulation of CO_2 in the water column (Marx et al., 2017). Additionally, higher temperatures during the dry season facilitate increased microbial decomposition of organic matter, further contributing to the elevated pCO_2 (Inglima et al., 2009). These conditions lead to greater CO_2 retention in the upstream sections of the river, as evidenced by the spatial trend where pCO_2 values decrease from upstream to downstream. This downstream decrease is likely due to CO_2 outgassing as the water travels, along with potential uptake by aquatic plants and algae, which reduces the overall pCO_2 concentration.

To better understand the factors influencing carbon dynamics in the Lianjiang River, Pearson correlation coefficients were calculated for key river water parameters and are summarized in Table S1. During the rainy season, there was a significant positive correlation ($p < 0.01$) with a high correlation coefficient (R^2 = 0.927 and 0.927, respectively) between pH and the saturation indices for calcite (SI_C) and dolomite (SI_D). This indicates that higher pH levels are associated with increased saturation of these carbonate minerals, which is typical in alkaline conditions where carbonate precipitation is more favorable. A strong negative correlation ($p < 0.01$) with a high correlation coefficient was found between pH and pCO_2, suggesting that increased CO_2 concentrations are linked to lower pH levels. This is consistent with the acidifying effect of CO_2 in water, where it forms carbonic acid, subsequently lowering the pH. This relationship is crucial during the rainy season when the river experiences higher pCO_2 levels due to runoff from CO_2^- rich soils and decaying organic matter. Furthermore, SI_C and SI_D exhibited a significant positive correlation ($p < 0.01$) with the highest correlation coefficient (R^2 = 1.00), indicating that calcite and dolomite saturation states are closely linked and likely governed by similar geochemical processes. Negative correlations ($p < 0.05$) between SI_C, SI_D, and pCO_2 were also observed, suggesting that as CO_2 levels rise, the river becomes less saturated with respect to these minerals, inhibiting their precipitation and favoring dissolution.

In the dry season, strong positive correlations ($p < 0.01$) with high correlation coefficients ($R^2 > 0.9$)

were observed between pH and SI_C, and pH and SI_D, reflecting that even during periods of low flow and high CO_2 concentrations, higher pH levels still promote carbonate mineral saturation. However, the negative correlations ($p < 0.05$) with high correlation coefficients ($R^2 > 0.7$) between pH, DIC, and pCO_2 highlight the complex interplay between DIC and CO_2, where increased CO_2 levels contribute to higher DIC concentrations but simultaneously lower pH, reducing carbonate saturation.

Additionally, positive correlations ($p < 0.05$) were observed between DIC and $\delta^{13}C_{DIC}$, as well as DIC and pCO_2, suggesting that $\delta^{13}C_{DIC}$ values are influenced by the sources and processes controlling DIC, including the balance between biogenic and geogenic CO_2 inputs. This implies that the isotopic composition of $\delta^{13}C_{DIC}$ is closely tied to the amount and source of CO_2 in the river, with heavier carbon isotopes becoming more prevalent as DIC concentrations increase, particularly during the dry season when biogenic CO_2 contributions are more dominant. These correlations and patterns underscore the distinct seasonal shifts in carbon dynamics within the Lianjiang River, driven by variations in water chemistry, flow regimes, and biological activity. The higher pCO_2 values during the dry season reflect a greater retention of CO_2 due to reduced flow and enhanced microbial activity, while the correlations between pH, SI_C, SI_D, and pCO_2 reveal the sensitivity of carbonate chemistry to CO_2 fluctuations and the overall impact of seasonal hydrological changes on the river's carbon cycle.

Distinct temporal and spatial differences in the pCO_2 pattern were observed between the upper and lower reaches of the Lianjiang River, reflecting the influence of varying hydrological and biogeochemical processes across the river's course. In the headwaters during the dry season, the highest pCO_2 values were recorded, indicating a significant contribution of soil-derived CO_2. This is likely due to reduced flow rates and increased water-soil interaction, which allows for more extensive contact between river water and CO_2^- rich soils. Soil CO_2, generated through microbial respiration and root respiration, diffuses into the river, leading to elevated pCO_2 levels, especially in the dry season when the solubility of CO_2 is enhanced by lower temperatures (Zavadlav et al., 2013). This contrasts with the rainy season, where increased runoff dilutes the concentration of soil-derived CO_2, resulting in lower pCO_2 values overall. The spatial distribution of pCO_2 along the river shows a clear decreasing trend from upstream to downstream, suggesting that as the river water travels downstream, CO_2 is progressively lost to the atmosphere through outgassing. This pattern is further supported by the observed increase in the saturation indices for calcite (SI_C) and dolomite (SI_D) from upstream to downstream. As CO_2 is lost from the water, the pH tends to increase, promoting the saturation of carbonate minerals. This process is more pronounced in the dry season, where the reduced flow and higher residence time in the river enhance CO_2 loss and carbonate saturation. A clear seasonal pattern in mineral saturation was also identified: the water in the Lianjiang River is highly saturated with respect to both calcite and dolomite during the rainy season, leading to the precipitation of these minerals (Figure 4). This is driven by higher temperatures and increased biological activity, which elevate pH and promote carbonate saturation. In contrast, during the dry season, the river becomes undersaturated with respect to both calcite and dolomite, leading to the dissolution of these minerals. This seasonal shift from precipitation to dissolution is likely driven by the combined effects of lower temperatures, reduced flow rates, and increased CO_2 levels, which together lower pH and reduce carbonate saturation.

The relationship between pCO_2 and carbonate saturation is complex, as indicated by the higher negative correlation between pCO_2 and SI_C, as well as pCO_2 and SI_D. Although CO_2 losses contribute to an increase in the carbonate saturation state of the river water, the conditions necessary for significant calcite precipitation are not fully met during the dry season. For calcite precipitation to occur in surface waters, a high oversaturation of $SI_C > 0.6$ is required (Merz-Preiß and Riding, 1999). However, the Lianjiang River rarely achieves this level of oversaturation during the dry season, making calcite precipitation unlikely. The observed CO_2 losses and their impact on carbonate chemistry suggest that the decrease in pCO_2 levels cannot be solely attributed to calcite precipitation. Other processes, such as CO_2 outgassing and biological uptake, likely play a more

significant role in regulating CO_2 levels and the overall carbonate balance in the river. Outgassing is particularly effective in the dry season, when reduced flow and increased water-air interface area enhance CO_2 transfer from the water to the atmosphere. Additionally, photosynthetic activity by aquatic plants and algae may contribute to CO_2 uptake, further reducing pCO_2 levels downstream.

These findings highlight the dynamic interplay between hydrological, biological, and geochemical processes in controlling the carbon cycle in the Lianjiang River. The seasonal and spatial variations in pCO_2, coupled with the changes in carbonate mineral saturation, underscore the complexity of the river's carbon dynamics and the importance of considering multiple processes when evaluating carbon transfer and storage in fluvial systems.

Contributions of different DIC sources. The potential sources of dissolved inorganic carbon (DIC) in the Lianjiang River Basin are primarily atmospheric CO_2, soil CO_2, and the dissolution of carbonate minerals. In this study, the pCO_2 in Lianjiang River water was much higher than atmospheric CO_2 ($p < 0.01$), indicating that the potential sources of DIC can only include soil CO_2 and the dissolution of carbonate minerals. Notably, significant differences in the $\delta^{13}C_{DIC}$ values of the river water samples suggest distinct contributions from DIC sources ($p > 0.05$). A qualitative assessment of the relative proportions of soil-derived carbon (f_{soil}) and rock-derived carbon (f_{carb}) in the groundwater studied can be expressed as (Schiavo et al., 2007).

$$\delta^{13}C_{DIC} = f_{soil}\left(\delta^{13}C_{CO_2(g)} - \varepsilon^{13}C_{CO_2(g)-HCO_3^-}\right) + f_{carb}\left(\delta^{13}C_{CaCO_3(s)} - \varepsilon^{13}C_{HCO_3^- - CaCO_3(s)}\right) \quad (1)$$

where f_{soil} and f_{carb} are the ratios of each end-member.

In this study, the stable carbon isotopes in soil ($\delta^{13}C_{soil}$) ranged from −26.7 ‰ to −19.2 ‰ with an average value of −23.0 ‰, indicating that the Lianjiang River Basin is predominantly covered by C_3 plant species, which is consistent with reality. The stable carbon isotopes in carbonate rocks ($\delta^{13}C_{rock}$) ranged between −1.2 ‰ and +3.3 ‰ with an average value of +1.63 ‰, as shown in Figure 5. The DIC contributions from carbonate weathering (f_{carb}) ranged from 37.1% to 47.8% with an average of 42.6% in the rainy season, while in the dry season, the contribution from f_{carb} ranged from 44.6% to 54.5% with an average of 49.9%. It can be observed that the DIC contributions from soil CO_2 (f_{soil}) were higher than f_{carb} in the rainy season, while very similar contributions were found between f_{soil} and f_{carb} in the dry season. According to the related study, the DIC contributions of carbonates (f_{carb}) are about 50% in groundwater (Jiang et al., 2013), which favors CO_2 dissolution under a closed system (Mook et al., 1974).

In addition, the stable isotope analysis results of δ^2H and $\delta^{18}O$ suggested that the Lianjiang River water was significantly recharged by adjacent groundwater. This was indicated by the similarity in isotopic signatures between the river water and local groundwater, implying a strong hydraulic connection between the two. The isotopic composition of the river water in the dry season closely matched that of the groundwater, confirming that the river is primarily fed by groundwater during this period. This groundwater recharge plays a critical role in sustaining river flow during the dry season, when surface runoff is minimal.

The DIC in the river also reflects contributions from carbonate dissolution and soil CO_2, with the isotope results indicating similar proportions from both sources. However, the contribution of carbonate dissolution to riverine DIC was observed to be lower in the rainy season compared to the dry season. This difference is likely due to the dilution effect of increased surface runoff during the rainy season, which reduces the relative contribution of carbonate dissolution. In contrast, during the dry season, the river receives a higher proportion of DIC from adjacent karst water, which is rich in carbonate minerals, leading to an increase in DIC derived from carbonate dissolution.

Carbon isotope fractionation processes also play a crucial role in influencing riverine $\delta^{13}C_{DIC}$ values. Fractionation occurs during various processes such as photosynthesis, respiration, and CO_2 exchange with the atmosphere, each of which can either enrich or deplete the riverine DIC in $\delta^{13}C_{DIC}$. These biological activities have bidirectional impacts on $\delta^{13}C_{DIC}$,

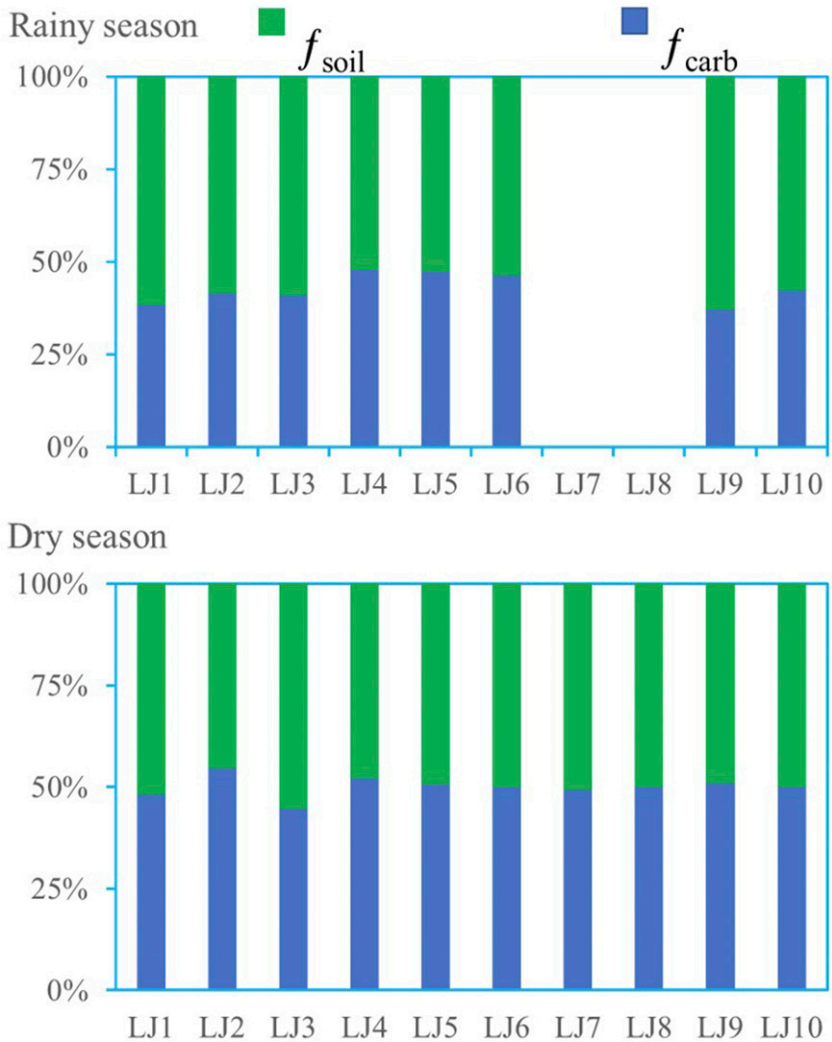

Figure 5. DIC contributions from carbonates weathering (f_{carb}) and soil CO_2 (f_{soil}) in river water between rainy season and dry season. For interpretation of the references to colours in this figure legend, refer to the online version of this article.

introducing complexities in estimating the exact sources of DIC. For example, high rates of photosynthesis during daylight hours can increase $\delta^{13}C_{DIC}$ values, while respiration at night or in deeper waters may lower them. Such diurnal variations, along with seasonal changes, make it challenging to precisely quantify the contributions from carbonate dissolution and other sources. Additionally, CO_2 exchange with the atmosphere can further alter $\delta^{13}C_{DIC}$ values, particularly in areas where the river is actively degassing CO_2.

In conclusion, while carbonate dissolution is a significant source of DIC in the Lianjiang River, particularly during the dry season, the observed variations in $\delta^{13}C_{DIC}$ highlight the influence of multiple interacting processes, including groundwater recharge, biological activity, and atmospheric exchange. Understanding these processes and their impact on carbon isotopes is essential for accurately assessing the carbon dynamics and sources of DIC in the river, especially when considering the seasonal shifts in hydrological and biogeochemical conditions.

Spatiotemporal variation and sources of n-alkanes

Compositions and distribution of n-alkanes. The n-alkanes were observed to range from C_{10} to C_{34} in both dissolved organic matter (DOM) and particulate organic matter (POM) samples. The total concentrations of n-alkanes in DOM ranged from 411 to 9035 ng/L, with an average concentration of 4370 ng/L. The total concentrations of n-alkanes in POM varied between 5224 and 15,211 ng/L, with an average concentration of 7986 ng/L. The results indicated that the total n-alkane concentrations in POM were generally higher than those in DOM. However, there was no apparent spatial variation observed in the total n-alkane concentrations in either POM or DOM samples from upstream to downstream.

In the DOM samples, the relative contribution of anthropogenic n-alkanes ranged from 33.5% to 60.6%, with an average of 47.6%, while the relative contribution of anthropogenic n-alkanes in POM samples ranged from 29.6% to 64.3%, with an average of 42.8%. On the other hand, the relative contribution of biogenic n-alkanes in DOM samples varied from 10.2% to 35.8%, with an average of 12.1%, whereas in POM samples, it varied from 19.1% to 41.5%, with an average of 31.2% (Figure 6). Overall, the average relative contribution of anthropogenic n-alkanes was found to be higher than that of biogenic n-alkanes in DOM samples, particularly when compared to POM samples. Furthermore, the average relative contribution of biogenic n-alkanes in POM samples was higher than that in DOM samples. But no significant spatial distribution characteristic was observed from upstream to downstream in the Lianjiang River.

N-alkanes sources identification in DOM and POM. It was reported that when the value of CPI is close to 1 n-alkanes prefer anthropogenic sources (Liu et al., 2022; Xu et al., 2017). In this study, the $CPI_{10\text{-}34}$ values of the Lianjiang River water in DOM ranged from 0.6 to 1.5, with a median value of 1.0 ± 0.3, while $CPI_{10\text{-}34}$ values in POM ranged from 1.4 to 3.6, with a median of 2.0 ± 1.1 (Figure 7(a)). These results suggest that anthropogenic activities are the predominant sources of organic matter in the industrial section of the mainstream Lianjiang River. Moreover, it is known that higher $CPI_{H\ (>C25)}$ values (>5) are typically associated with terrestrial organic matter (Bray and Evans, 1961). Therefore, the higher $CPI_{21\text{-}34}$ values (>5) observed in POM samples collected from sites LJ3 and LJ5 suggest that terrestrial organic matter was the primary source of POM in these locations.

As shown in Figure 7(b), there was a significant negative correlation ($p < .01$) between $CPI_{10\text{-}34}$ and $CPI_{21\text{-}34}$, $CPI_{10\text{-}20}$ and $CPI_{21\text{-}34}$ in DOM samples. Additionally, $CPI_{10\text{-}34}$ in DOM samples exhibited a higher positive correlation ($p < 0.05$) with $CPI_{10\text{-}20}$ in DOM samples. These findings support the notion that terrestrial organic matter, particularly vascular plants or other higher plants, was not a major source of organic matter in both POM and DOM samples, as indicated by the analysis of CPI values.

To determine the contributions of different biogenic sources, biogenic ACL (ACL_{bio}) was used (Table S2). Previous studies have shown that ACL_{bio}<21 is indicative of a dominant source of algae, while ACL_{bio}>26 suggests a predominant source of terrestrial plants. ACL_{bio} values falling between 21 and 26 represent a mixture of algae and terrestrial plants (He et al., 2020; Sikes et al., 2009). The P_{aq} index is used to determine the relative contributions of terrestrial and freshwater plants and can be divided into three categories: <0.1, 0.1–0.4, and 0.4–1. A P_{aq} index value of <0.1 indicates a dominant contribution from terrestrial plants, while a value of 0.1–0.4 suggests a significant contribution from aquatic macrophytes, and a value of 0.4–1 indicates a substantial contribution from floating and submerged aquatic plants (Ficken et al., 2000b; Zhao et al., 2022). In this study, the ACLbio values in DOM samples ranged from 12.4 to 28.2, with a median value of 18.2, while in POM samples, the values varied from 15.7 to 27.5, with a median value of 18.9. The lower ACL_{bio} values observed in both DOM and POM samples suggest that algae is the primary source of biogenic n-alkanes in Lianjiang River during the dry season. However, the P_{aq} values in DOM samples ranged from 0 to 0.96, while in POM samples, they varied from 0.13 to 1.0, indicating that biogenic n-alkanes in Lianjiang River

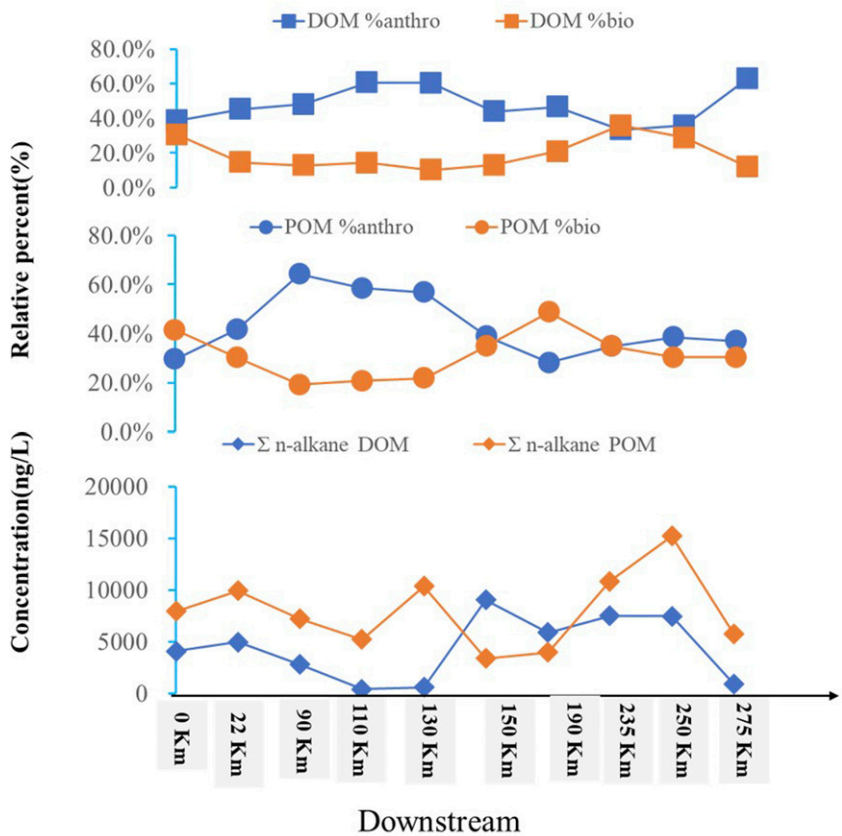

Figure 6. Variations in relative contribution of $\Sigma_{biogenic}$ n-alkanes (DOM, POM), $\Sigma_{anthropogenic}$ n-alkanes (DOM, POM), and $\Sigma_{n\text{-}alkane}$ concentrations (DOM, POM) in river waters. For interpretation of the references to colours in this figure legend, refer to the online version of this article.

originate from multiple sources. These results are contrary to previous findings based on ACL_{bio} values. As shown in Figure 8, the ACL_{bio} values in both DOM and POM samples can be categorized into two groups: ACL_{bio} values lower than 20 and ACL_{bio} values higher than 24. The sampling sites that fall under the latter category include site LJ6 in POM and sites LJ4, LJ5, and LJ10 in DOM. Most of the sampling sites in POM samples belong to the group with $ACL_{bio}<20$. Based on these results, it can be concluded that algae, as well as floating and submerged aquatic plants, were the primary sources of biogenic n-alkanes in Lianjiang River water, particularly in POM samples.

Previous studies have demonstrated that short-chain anthropogenic n-alkanes are effective tracers for light petroleum sources, such as gasoline and diesel, whereas long-chain anthropogenic n-alkanes are typically associated with heavy soils or the incomplete combustion of fossil fuels at high temperatures (Kang et al., 2018; Lichtfouse et al., 1997; Liu et al., 2022; Wang et al., 2018). In this study, the peaks of short-chain and long-chain homologs were identified using C1 and C2, respectively. The C1/C2 ratio was then utilized to assess the carbon-chain distribution of anthropogenic n-alkanes. A C1/C2 ratio greater than 1 indicates a predominance of light petroleum sources, while a ratio less than 1 suggests a preference for heavy oil emissions or incomplete fossil fuel combustion (Liu et al., 2022). As shown in Figure 9(a), the C1/C2 ratios in DOM samples ranged from 0.14 to 3.27, with a median value of 2.58,

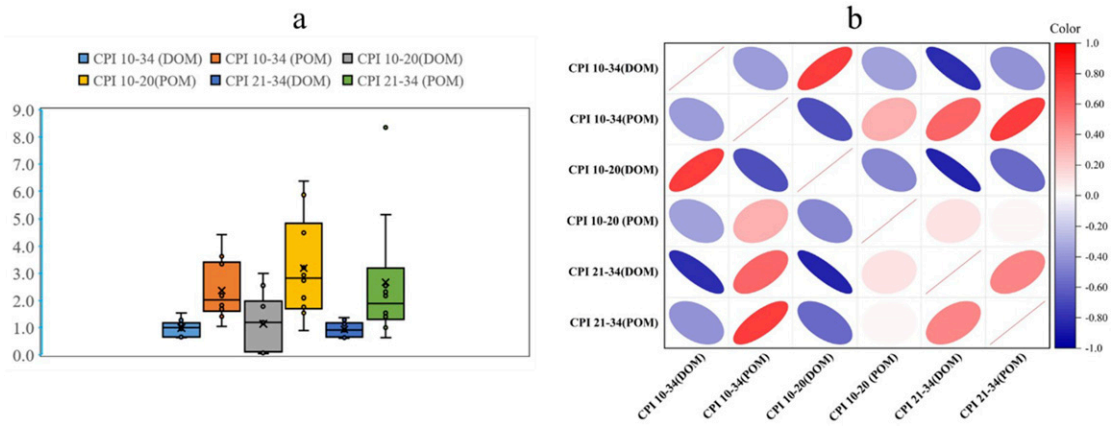

Figure 7. Box plots of CPIs (a) and their correlations (b) in Lianjiang River. For interpretation of the references to colours in this figure legend, refer to the online version of this article.

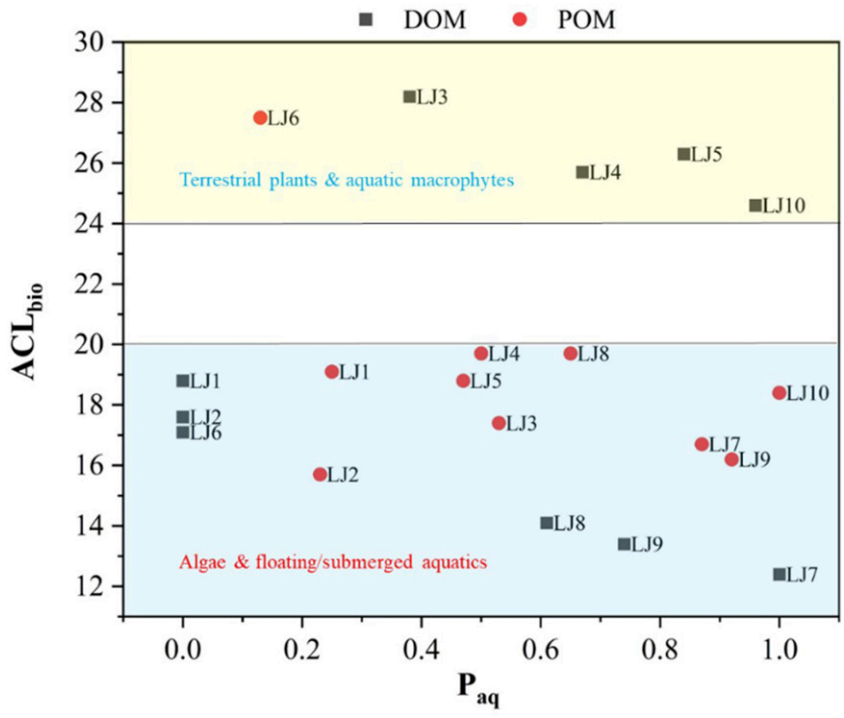

Figure 8. Plots of the P_{aq} versus ACL_{bio} showing the potential sources of biogenic n-alkanes in DOM and POM. For interpretation of the references to colours in this figure legend, refer to the online version of this article.

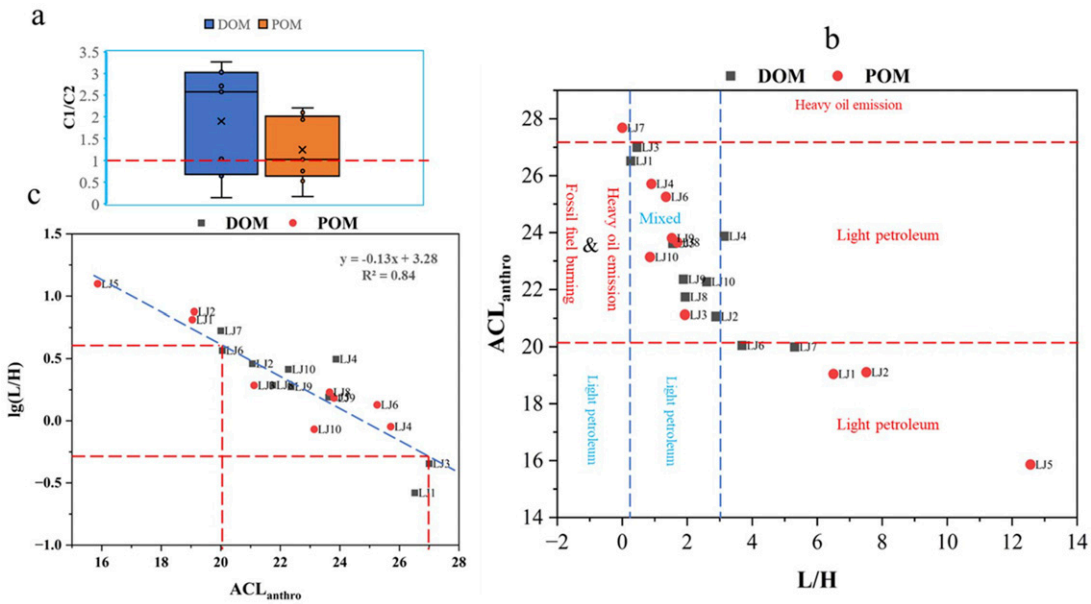

Figure 9. Source diagnosis of anthropogenic n-alkanes by using C1/C2, L/H and ACL_{anthro}. For interpretation of the references to colours in this figure legend, refer to the online version of this article.

suggesting that anthropogenic n-alkanes in DOM were primarily derived from light petroleum sources. In contrast, the C1/C2 ratios in POM samples ranged from 0.52 to 2.20, with a median value of 1.0, which was significantly lower than that observed in DOM samples. This lower ratio in POM samples indicates a stronger influence from incomplete fossil fuel combustion or heavy oil emissions. The higher occurrence of short-chain homologs in POM samples may be related to the adsorption characteristics of POM in river water, as higher-chain homologs are more readily absorbed by POM.

In this study, the anthropogenic Average Chain Length (ACL_{anthro}) and the ratio of unit short-to-long carbon anthropogenic n-alkanes (L/H) were employed to quantify the contributions of different anthropogenic sources (Liu et al., 2022). As illustrated in Figure 9(c), there is a strong negative correlation ($p < 0.01$) between lg (L/H) and ACL_{anthro}, confirming the effectiveness of these proxies in assessing the quantitative contributions of various sources. Based on Figure 9(b), we propose that an lg (L/H) value greater than 0.57 corresponds to an ACL_{anthro} of less than 20, indicating a predominance of light petroleum inputs. Conversely, an lg (L/H) value below −0.34 corresponds to an ACL_{anthro} greater than 27, suggesting a dominance of incomplete fossil fuel combustion at high temperatures and heavy oil emissions. Values falling between −0.34 and 0.57 ($20 < ACL_{anthro} < 27$) indicate a mixture of sources. Therefore, the anthropogenic sources in the Lianjiang River are primarily derived from a combination of light petroleum inputs and incomplete fossil fuel combustion at high temperatures, along with heavy oil emissions.

Conclusions

In this study, we have examined the spatiotemporal variations in DOC, DIC, and pCO_2 concentrations, along with the isotopic compositions of DIC, to understand how these factors are influenced by the hydrological regimes in the Lianjiang River mainstream. Our findings underscore the intricate interplay between hydrological changes and carbon dynamics in river systems, offering new insights into the sources and processes governing DIC and DOC concentrations. We observed that during the dry season, the Lianjiang River's water was primarily

recharged by groundwater, while in the rainy season, soil CO_2 emerged as the dominant contributor to DIC. This seasonal variation highlights the critical role of hydrological processes in shaping riverine carbon dynamics. The positive correlation between $\delta^{13}C_{DIC}$ and DIC concentrations further emphasizes the influence of groundwater discharge during the dry season, while the decrease in pCO_2 concentrations suggests significant CO_2 degassing along the river, particularly in the dry season.

Our findings also reveal that while DOC concentrations were relatively stable across seasons and spatial scales, the sources of n-alkanes in the Lianjiang River showed marked differences. The dominance of anthropogenic n-alkanes in both POM and DOM, particularly from light petroleum and fossil fuel combustion, points to ongoing anthropogenic impacts on the river's carbon cycle. The identification of algae, aquatic plants, and terrestrial inputs as primary sources of biogenic n-alkanes further enriches our understanding of organic matter dynamics in this riverine system.

The implications of our study extend beyond the Lianjiang River, offering valuable lessons for managing and preserving riverine ecosystems in the face of changing hydrological conditions. As rivers worldwide are increasingly impacted by human activities and climate change, it is imperative that future research and conservation efforts consider the complex interactions between hydrology, carbon dynamics, and anthropogenic influences. Additionally, ongoing monitoring of isotopic compositions and organic matter sources is crucial for understanding and managing the evolving dynamics of carbon in river systems. By focusing on these aspects, we hope this study contributes to the broader understanding of riverine carbon dynamics and serves as a foundation for further research and action in the field.

Acknowledgments

I would like to express my deepest gratitude to Dr. Xiao Yanan for her invaluable support during the preparation of this article. Her expertise in data analysis methodologies provided critical guidance throughout the research process. I am truly honored to have benefited from her mentorship.

Declaration of conflicting interests

The author(s) declared no potential conflicts of interest with respect to the research, authorship, and/or publication of this article.

Funding

Guangxi Key Science and Technology Innovation Based on Karst Dynamics (KDL & Guangxi 202012, KDL & Guangxi 202105), Natural Science Foundation of Guangdong Province of China (2021A1515110505), National Natural Science Foundation of China (42302269), Natural Science Foundation of Guangxi China (2023JA150068).

ORCID iD

Zuobing Liang https://orcid.org/0000-0002-0662-7838

Supplemental Material

Supplemental material for this article is available online.

References

Andersson AJ, Mackenzie FT and Ver LM (2003) Solution of shallow-water carbonates: an insignificant buffer against rising atmospheric CO2. *Geology* 31: 513–516.

Armstrong A (2012) Riverine carbon unravelled. *Nature Geoscience* 5: 684.

Bauer JE, Cai W-J, Raymond PA, et al. (2013) The changing carbon cycle of the coastal ocean. *Nature* 504: 61–70.

Beaulieu E, Goddéris Y, Donnadieu Y, et al. (2012) High sensitivity of the continental-weathering carbon dioxide sink to future climate change. *Nature Climate Change* 2: 346–349.

Bianchi TS (2011) The role of terrestrially derived organic carbon in the coastal ocean: a changing paradigm and the priming effect. *Proceedings of the National Academy of Sciences* 108: 19473–19481.

Blair NE and Aller RC (2012) The fate of terrestrial organic carbon in the marine environment. *Annual Review of Marine Science* 4: 401–423.

Bray EE and Evans ED (1961) Distribution of n-paraffins as a clue to recognition of source beds. *Geochimica et Cosmochimica Acta* 22: 2–15.

Caumo S, Bruns RE and Vasconcellos PC (2020) Variation of the distribution of atmospheric n-alkanes emitted by different fuels' combustion. *Atmosphere* 11: 643.

Chen B, Zhao M, Yan H, et al. (2021) Tracing source and transformation of carbon in an epikarst spring-pond system by dual carbon isotopes (13C14C): evidence of dissolved CO2 uptake as a carbon sink. *Journal of Hydrology* 593: 125766.

Cole JJ, Prairie YT, Caraco NF, et al. (2007) Plumbing the global carbon cycle: integrating inland waters into the terrestrial carbon budget. *Ecosystems* 10: 172–185.

Derrien M, Yang LY and Hur J (2017) Lipid biomarkers and spectroscopic indices for identifying organic matter sources in aquatic environments: a review. *Water Research* 112: 58–71.

Ficken KJ, Li B, Swain DL, et al. (2000a) An *n*-alkane proxy for the sedimentary input of submerged/floating freshwater aquatic macrophytes. *Organic Geochemistry* 31: 745–749.

Ficken KJ, Li B, Swain DL, et al. (2000b) An n-alkane proxy for the sedimentary input of submerged/floating freshwater aquatic macrophytes. *Organic Geochemistry* 31: 745–749.

Gao Q and Wang Z (2015) Dissolved inorganic carbon in the Xijiang River: concentration and stable isotopic composition. *Environmental Earth Sciences* 73: 253–266.

Gat JR, Shemesh A, Tziperman E, et al. (1996) The stable isotope composition of waters of the eastern Mediterranean Sea. *Journal of Geophysical Research* 101: 6441–6451.

Ge T, Xue Y, Jiang X, et al. (2020) Sources and radiocarbon ages of organic carbon in different grain size fractions of Yellow River-transported particles and coastal sediments. *Chemical Geology* 534: 119452.

Hao Z, Gao Y, Ma MZ, et al. (2019) Using $\delta^{13}C$ to reveal the importance of different water transport pathways in two nested karst basins, Southwest China. *Journal of Hydrology* 571: 425–436.

He Y, Yang C, He W, et al. (2020) New insights into spatiotemporal source apportionment of n-alkanes under mixed scenario: a pilot study on Lake Chaohu, China. *The Science of the Total Environment* 742: 140517.

Inglima I, Alberti G, Bertolini T, et al. (2009) Precipitation pulses enhance respiration of Mediterranean ecosystems: the balance between organic and inorganic components of increased soil CO2 efflux. *Global Change Biology* 15: 1289–1301.

Jiang Y, Hu Y and Schirmer M (2013) Biogeochemical controls on daily cycling of hydrochemistry and δ13C of dissolved inorganic carbon in a karst spring-fed pool. *Journal of Hydrology* 478: 157–168.

Kang M, Ren L, Ren H, et al. (2018) Primary biogenic and anthropogenic sources of organic aerosols in Beijing, China: insights from saccharides and n-alkanes. *Environmental Pollution* 243: 1579–1587.

Khadka MB, Martin JB and Jin J (2014) Transport of dissolved carbon and CO2 degassing from a river system in a mixed silicate and carbonate catchment. *Journal of Hydrology* 513: 391–402.

Larsen LG, Aiken GR, Harvey JW, et al. (2010) Using fluorescence spectroscopy to trace seasonal DOM dynamics, disturbance effects, and hydrologic transport in the Florida Everglades. *Journal of Geophysical Research: Biogeosciences* 115: G03001.

Li Q, Sun H, Han J, et al. (2008) High-resolution study on the hydrochemical variations caused by the dilution of precipitation in the epikarst spring: an example spring of Landiantang at Nongla, Mashan, China. *Environmental Geology* 54: 347–354.

Li J, Pang Z, Froehlich K, et al. (2015) Paleo-environment from isotopes and hydrochemistry of groundwater in east junggar basin, northwest China. *Journal of Hydrology* 529: 650–661.

Liang Z, Li S, Wang Z, et al. (2022) Microbial community structure characteristics among different karst aquifer systems, and its potential role in modifying hydraulic properties of karst aquifers. *Frontiers in Microbiology* 13: 1054295.

Lichtfouse É, Bardoux G, Mariotti A, et al. (1997) Molecular, 13C, and 14C evidence for the allochthonous and ancient origin of C16-C18 n-alkanes in modern soils. *Geochimica et Cosmochimica Acta* 61: 1891–1898.

Liu JK and Han GL (2020) Effects of chemical weathering and CO_2 outgassing on $\delta^{13}C_{Dic}$ signals in a karst watershed. *Journal of Hydrology* 589: 125192.

Liu Z, Macpherson GL, Groves C, et al. (2018) Large and active CO2 uptake by coupled carbonate weathering. *Earth-Science Reviews* 182: 42–49.

Liu Z, Yuan Y, Jaimeewong P, et al. (2018) Synthesis, structure, dielectric properties and relaxor behavior of

a novel solid solution (1-x)Pb(Mg1/3Nb2/3)O3-xBi(Zn2/3Nb1/3)O3. *Ferroelectrics* 534: 42–49.

Liu Y, He Y, Liu Y, et al. (2022) Assessing spatiotemporal sources of biogenic and anthropogenic sedimentary organic matter from the mainstream Haihe River, China: using n-alkanes as indicators. *The Science of the Total Environment* 834: 155382.

Marx A, Dusek J, Jankovec J, et al. (2017) A review of CO2 and associated carbon dynamics in headwater streams: a global perspective. *Reviews of Geophysics* 55: 560–585.

Mayorga E, Aufdenkampe AK, Masiello CA, et al. (2005) Young organic matter as a source of carbon dioxide outgassing from Amazonian rivers. *Nature* 436: 538–541.

McDonough LK, Andersen MS, Behnke MI, et al. (2022) A new conceptual framework for the transformation of groundwater dissolved organic matter. *Nature Communications* 13: 2153.

Merz-Preiß M and Riding R (1999) Cyanobacterial tufa calcification in two freshwater streams: ambient environment, chemical thresholds and biological processes. *Sedimentary Geology* 126: 103–124.

Mook WG, Bommerson JC and Staverman WH (1974) Carbon isotope fractionation between dissolved bicarbonate and gaseous carbon dioxide. *Earth and Planetary Science Letters* 22: 169–176.

Peterson BJ and Fry B (1987) Stable isotopes in ecosystem studies. *Annual Review of Ecology and Systematics* 18: 293–320.

Pu JB, Yuan DX, Zhao HP, et al. (2014) Hydrochemical and PCO_2 variations of a cave stream in a subtropical karst area, Chongqing, SW China: piston effects, dilution effects, soil CO_2 and buffer effects. *Environmental Earth Sciences* 71: 4039–4049.

Schiavo MA, Hauser S and Povinec PP (2007) Isotope distribution of dissolved carbonate species in southeastern coastal aquifers of Sicily (Italy). *Hydrological Processes* 21: 2690–2697.

Sikes EL, Uhle ME, Nodder SD, et al. (2009) Sources of organic matter in a coastal marine environment: evidence from n-alkanes and their δ13C distributions in the Hauraki Gulf, New Zealand. *Marine Chemistry* 113: 149–163.

Singh S, Inamdar S, Mitchell M, et al. (2014) Seasonal pattern of dissolved organic matter (DOM) in watershed sources: influence of hydrologic flow paths and autumn leaf fall. *Biogeochemistry* 118: 321–337.

Sun H, Han J, Zhang S, et al. (2015) Carbon isotopic evidence for transformation of DIC to POC in the lower Xijiang River, SE China. *Quaternary International* 380-381: 288–296.

Wang X, Ma H, Li R, et al. (2012) Seasonal fluxes and source variation of organic carbon transported by two major Chinese Rivers: the Yellow River and Changjiang (Yangtze) River. *Global Biogeochemical Cycles* 26: GB2025.

Wang S, Liu G, Yuan Z, et al. (2018) n-Alkanes in sediments from the Yellow River Estuary, China: occurrence, sources and historical sedimentary record. *Ecotoxicology and Environmental Safety* 150: 199–206.

Wigley T (1977) WATSPEC: a computer program for determining the equilibrium speciation of aqueous solutions. *Geo-Abstracts for the British Geomorphological Research Group*.

Xu F-L, Yang C, He W, et al. (2017) Bias and association of sediment organic matter source apportionment indicators: a case study in a eutrophic Lake Chaohu, China. *The Science of the Total Environment* 581-582: 874–884.

Xue Y, Zou L, Ge T, et al. (2017) Mobilization and export of millennial-aged organic carbon by the Yellow River. *Limnology & Oceanography* 62: S95–S111.

Yang Y, Yuan X, Deng Y, et al. (2020) Seasonal dynamics of dissolved organic matter in high arsenic shallow groundwater systems. *Journal of Hydrology* 589: 125120.

Zavadlav S, Kanduč T, McIntosh J, et al. (2013) Isotopic and chemical constraints on the biogeochemistry of dissolved inorganic carbon and chemical weathering in the karst watershed of krka river (Slovenia). *Aquatic Geochemistry* 19: 209–230.

Zhao M, Sun H, Liu Z, et al. (2022) Organic carbon source tracing and the BCP effect in the Yangtze River and the Yellow River: insights from hydrochemistry, carbon isotope, and lipid biomarker analyses. *The Science of the Total Environment* 812: 152429.

Zheng M, Fang M, Wang F, et al. (2000) Characterization of the solvent extractable organic compounds in PM2.5 aerosols in Hong Kong. *Atmospheric Environment* 34: 2691–2702.